

NEW NON-LINEAR APPROACH FOR THE EVALUATION OF THE LINEARITY OF HIGH GAIN HARMONIC SELF-OSCILLATING MIXERS

M. Fernandez*, S. Ver Hoeye, C. Vazquez, G. Hotopan, R. Camblor, and F. Las Heras

Area of Signal Theory and Communications, Department of Electrical Engineering, University of Oviedo, Campus de Viesques, Edificio Polivalente s/n, Modulo 8, Planta 1, E-33203, Gijon, Spain

Abstract—In this work, the linearity of a high gain Harmonic Self Oscillating Mixer (HSOM) is analyzed. In order to obtain high conversion gain, the working point of the HSOM is established close to a Hopf bifurcation point. The traditional figures of merit used to characterize the linearity of conventional mixers cannot be directly applied to characterize the behavior of autonomous circuits, because of the influence of the input RF signal power on the autonomous signal parameters. The 1 dB compression point and the third order distortion will be analyzed as a function of the harmonic content and maximum gain of the circuit. From the collected data, the optimum harmonic content and the maximum conversion gain of the HSOM can be selected, for a particular application, in order to minimize the output IF signal distortion.

1. INTRODUCTION

Modern microwave communication systems, and specially wireless and portable implementations, have to comply with strict requirements about size, weight, power consumption and cost. These goals can be achieved by using multi-functional circuits, which enable the implementation of several blocks of the communication system using a reduced number of components. From this point of view, the Harmonic Self Oscillating Mixer (HSOM) is a multi-functional circuit which results an attractive option to be used in front-end stages of microwave

Received 10 January 2012, Accepted 2 March 2012, Scheduled 11 March 2012

* Corresponding author: Miguel Fernandez (mfgarcia@tsc.uniovi.es).

and millimetre-wave receivers. With a single transistor, the HSOM works as a mixer with positive conversion gain and generates the local oscillator signal.

In recent years, several techniques based on Harmonic Balance (HB) have been developed to design and analyze HSOM and other autonomous circuits by using commercial simulators [1–3]. These techniques are based on the use of an auxiliary generator and allow the control of the frequency and the harmonic content of the autonomous signal. However, they cannot deal with the main drawback of HSOM circuits, i.e., the high conversion losses and the narrow bandwidth.

In this work, the conversion gain of the HSOM will be considerably improved through the application of a recently developed technique based on bifurcation analysis and control methods [4]. This technique combines the control of the harmonic content of the autonomous signal [3] with the careful selection of the HSOM operating regime, which will be established in the vicinity of a Hopf bifurcation point [5–7]. Thus, the high amplification effect associated with this working point will be used in order to improve the conversion gain of the HSOM.

As in any amplifier [8–10], mixer [11–17], or active antenna with mixing capabilities [18], noise behavior [11,12] and IF signal distortion [13,18] are key factors that must be rigorously analyzed and minimized. In this work, it will be shown that the figures of merit which are traditionally used to analyze the linearity of conventional mixers cannot be directly applied to an autonomous circuit like the HSOM, because of the influence of the input RF signal power on the parameters of the self-oscillating signal. In this work, the distortion of the output signal will be analyzed versus the harmonic content of the autonomous signal and the working point of the circuit. Therefore, for each particular application, the optimum working parameters can be selected in order to reach a trade-off between the maximum allowed distortion and the required conversion gain.

This paper is organized as follows. In Section 2, the circuit topology and the design method, based on the use of an auxiliary generator, are described. The analysis of the conversion gain of the HSOM versus the harmonic content of the autonomous signal and the working regime is presented in Section 3. Finally, Section 4 provides an in-depth analysis of the linearity of the mixing operation, as a function of the harmonic content of the autonomous signal and the operation point of the circuit.

2. TOPOLOGY AND DESIGN OF THE HSOM

2.1. Topology

The topology of the HSOM is represented in Fig. 1. The circuit is based on a single ultra-low noise PHEMT transistor with a feedback network placed at the source terminal which provides the negative resistance required at the gate port for the start-up of the autonomous signal, with frequency $f_o = 3.25$ GHz and amplitude V_o . The feedback network includes a varactor which allows frequency tuning. The input RF signal, with center frequency $f_{RF} = 11.5$ GHz and power P_{RF} is connected to the gate port through a band-pass filter. A multi-harmonic load based on an arbitrarily width modulated transmission line [19] is also connected to the gate port of the transistor. The parameters of this load will be used along the entire design process in order to set the frequency and the harmonic content of the autonomous signal, as well as the working regime. The output IF signal, with center frequency $f_{IF} = f_{RF} - 3f_o = 1.75$ GHz is obtained through a mixing operation between the input RF signal and the third harmonic component of the autonomous signal. It is selected at the drain port of the transistor by means of a band-pass filter. The Auxiliary Generator (AG), connected at the gate port of the transistor, will be used to impose the frequency f_o and the harmonic content, i.e., the amplitudes of the fundamental V_o and the third V_o^3 harmonic components of the autonomous signal. A current source, with frequency f_p and very small amplitude $i_p = \epsilon$ is also connected to the gate port. This generator will be used to determine the working point of the HSOM.

An overview of the HSOM design, optimization and analysis processes is provided by the flow chart represented in Fig. 2, including the oscillator design process (a), the analysis of the conversion gain G_c versus the harmonic content of the autonomous signal (b), and the analysis of the conversion gain and the linearity of the mixing operation versus the working point of the HSOM (c). All these design, optimization and analysis steps will be described in detail in the next sections.

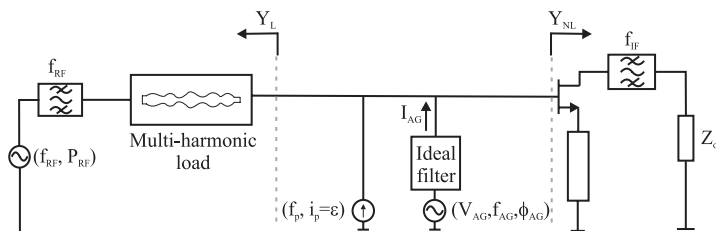


Figure 1. Topology of the Harmonic Self Oscillating Mixer.

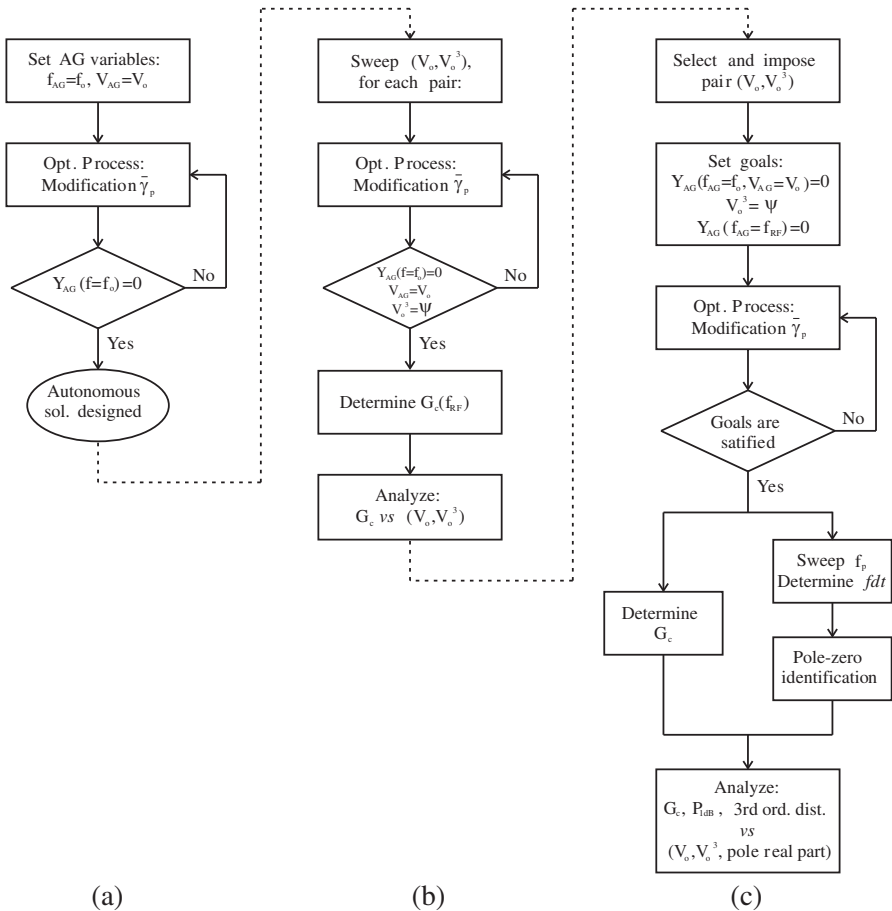


Figure 2. Overview of the design, optimization and analysis processes. (a) Design of the oscillator by means of an Auxiliary Generator (AG). (b) Analysis of the conversion gain G_c versus the harmonic content of the autonomous signal (V_o, V_o^3). (c) Analysis of the conversion gain and the linearity of the mixing operation versus the circuit working point.

2.2. Autonomous Solution of the HSOM

Several linear [20] and non linear methods, [21, 22], have been proposed to design and analyze microwave autonomous circuits. In this work, the auxiliary generator technique is used to set the autonomous solution of the HSOM [1–3, 23]. The auxiliary generator is connected at the gate port of the transistor and works with frequency $f_{AG} = f_o$ and

amplitude $V_{AG} = V_o$. The frequency f_o and the amplitude V_o of the fundamental harmonic component of the autonomous signal are imposed through an optimization process in which several parameters of the circuit, including those of the multi-harmonic load, are modified in order to satisfy the non-perturbation condition of the auxiliary generator $Y_{AG} = I_{AG}/V_{AG} = 0$ [1–3]. When this condition, expressed in terms of the real and imaginary parts of the admittance of the auxiliary generator, is fulfilled, the current through the auxiliary generator is zero. Therefore, no power is dissipated by or delivered to the circuit.

The auxiliary generator is also used to impose the amplitude V_o^3 of the third harmonic component of the autonomous signal. In this case, the corresponding condition is added to the set of goals that define the optimization process:

$$\begin{cases} Y_{AG}^r(f_{AG} = f_o, V_{AG} = V_o, \bar{\gamma}_p) = 0 \\ Y_{AG}^i(f_{AG} = f_o, V_{AG} = V_o, \bar{\gamma}_p) = 0 \\ |V_o^3(\gamma_p)| - \psi = 0 \end{cases} \quad (1)$$

where the superscripts (r) and (i) are used to denote the real and imaginary parts, $\bar{\gamma}_p$ is the set of circuit parameters involved in the optimization process and ψ is the desired amplitude of the third harmonic component of the autonomous signal. When all the three conditions expressed in (1) are fulfilled, the circuit is able to maintain an autonomous solution with frequency f_o and amplitudes of the fundamental and third harmonic components V_o and $V_o^3 = \psi$, respectively. Note the difference with respect to [3], where the amplitude of the desired harmonic component of the autonomous signal is imposed through a substitution generator.

3. CONVERSION GAIN OF THE HSOM

The auxiliary generator technique allows an accurate control over the frequency f_o and the harmonic content (V_o , V_o^3) of the autonomous signal of the HSOM. However, additional methods are required in order to improve the conversion gain of the circuit. In this work, the conversion gain will be enhanced through the application of a recently developed technique based on the independent control of the harmonic content of the autonomous signal and the working regime of the circuit [5–7].

3.1. Harmonic Content of the HSOM

In order to analyze the influence of the harmonic content of the autonomous signal on the conversion gain G_c of the HSOM, a double

sweep on the amplitudes of the fundamental and third harmonic components of the autonomous signal (V_o , $V_o^3 = \psi$) is performed. At each point of the sweep, which corresponds to a particular selection of the harmonic content, the optimization variables $\bar{\gamma}_p$ are modified in order to satisfy the non-perturbation condition of the auxiliary generator [1–3]. Note that, due to the coupling between the harmonic balance equations, this fact involves the compliance with the three conditions expressed in (1).

The amplitude of the first harmonic component of the autonomous signal has been changed between $V_o = 1$ V and $V_o = 1.5$ V. For each value of V_o , the amplitude of the third harmonic component of the autonomous signal has been varied from $V_o^3 = 0.05$ V to $V_o^3 = 0.3$ V. The result of the analysis is shown in Fig. 3. As can be observed, the conversion gain strongly depends on the amplitude of V_o^3 , since this harmonic component plays the role of local oscillator signal. On the other hand, if V_o is greater than 1.2 V, the shape of the conversion gain presents a considerably greater ripple along the considered frequency band, from $f_{RF} = 10.6$ GHz to $f_{RF} = 12.4$ GHz. Note that, the maximum conversion gain, evaluated at the center of the considered band, that can be obtained by controlling the circuit harmonic content is less than $G_c = -20$ dB.

From this analysis, the optimum pair (V_o , V_o^3) for each particular application can be selected. It should be taken into account that, in most cases, a trade-off between the maximum conversion gain and its ripple along the working frequency band should be attained.

3.2. Working Regime Close to a Hopf Bifurcation Point

As has been shown in the previous section, the maximum value of the conversion gain which can be reached by means of controlling of the harmonic content of the HSOM is about $G_c \approx -20$ dB. The conversion gain of the circuit will be improved through the selection of an adequate working point. When a non linear circuit works close to a Hopf bifurcation point, a high amplification effect is generated. This phenomenon has been described as undesired in [24], since it causes noise amplification over some spectral bands. However, it has also been shown that, when is carefully controlled, this phenomenon can be exploited to strongly amplify a weak signal [5–7].

The Hopf bifurcation point can be detected from the analysis of the transfer function of the nonlinear system, which is linearized around its steady state autonomous solution. The linearized transfer function of the system is calculated as the impedance seen by a perturbing current generator with small amplitude $i_p = \epsilon$, connected in parallel with the gate port of the transistor (see Fig. 1) [25]. At

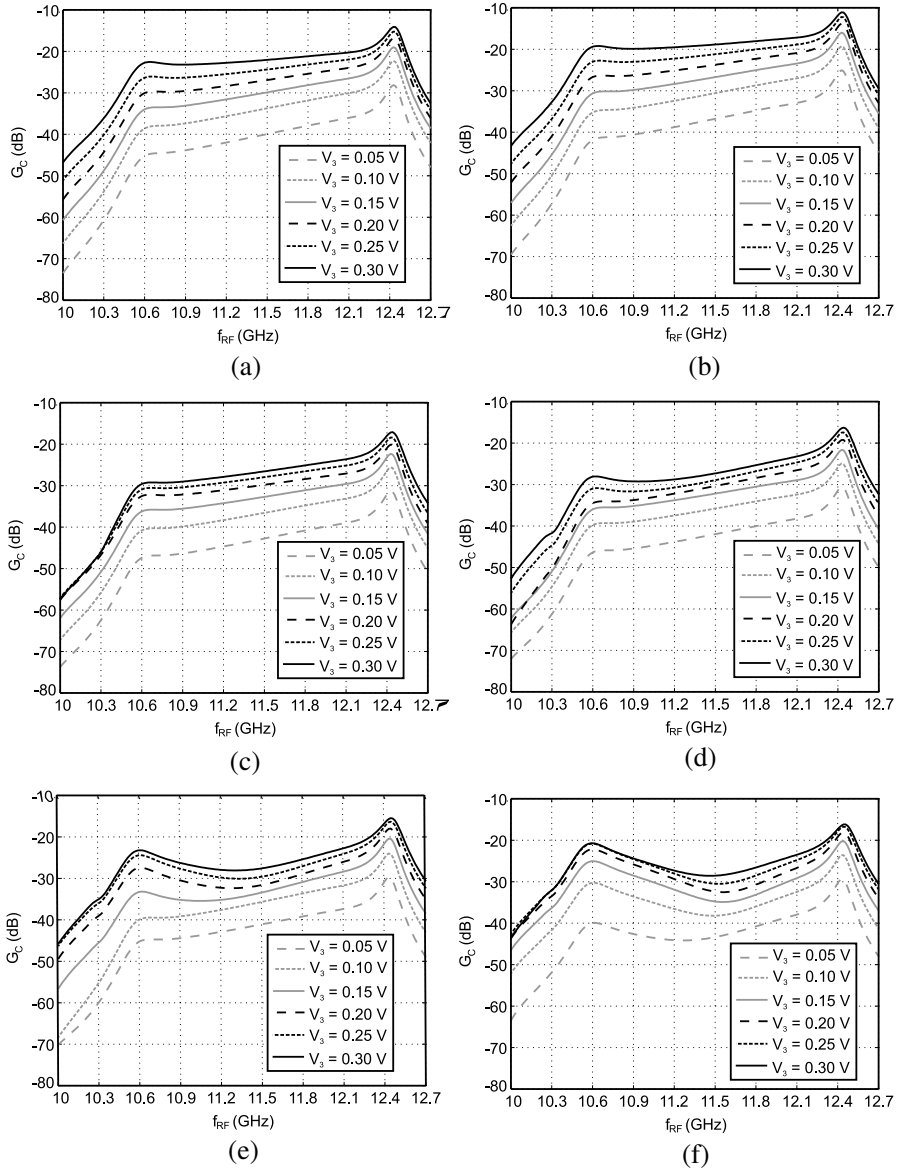


Figure 3. Conversion gain of the HSOM as a function of the harmonic content of the circuit. (a) $V_o = 0.9$ V. (b) $V_o = 1$ V. (c) $V_o = 1.1$ V. (d) $V_o = 1.2$ V. (e) $V_o = 1.3$ V. (f) $V_o = 1.4$ V.

the Hopf bifurcation point, a couple of complex conjugate poles, with negative real part, crosses the imaginary axis of the complex plane. The amplification effect which is generated is centered around the frequency of the pole pair, and its magnitude increases as the negative real part approaches zero. Note that the system is stable only if the real part of the poles is negative.

In order to improve the conversion gain of the HSOM, a pair of complex conjugate poles, with small negative real part, will be created around the center frequency of the input signal $f_{RF} = 11.5$ GHz. Hence, the amplification effect is used to enlarge the magnitude of the input RF signal. To set this operating point, the circuit is optimized in order to reach a quasi-zero admittance condition at the gate port of the transistor. This condition, which must be fulfilled around the center frequency of the input signal band, can be written as:

$$\begin{cases} Y_{AG}^r(f = f_{RF}) = Y_L^r(f = f_{RF}) + Y_{NL}^r(f = f_{RF}) \approx 0 \\ Y_{AG}^i(f = f_{RF}) = Y_L^i(f = f_{RF}) + Y_{NL}^i(f = f_{RF}) \approx 0 \end{cases} \quad (2)$$

where the admittance of the auxiliary generator Y_{AG} is expressed as the sum of the admittance that represents the linear part of the circuit, Y_L , and the admittance which represents its non linear part, Y_{NL} (see

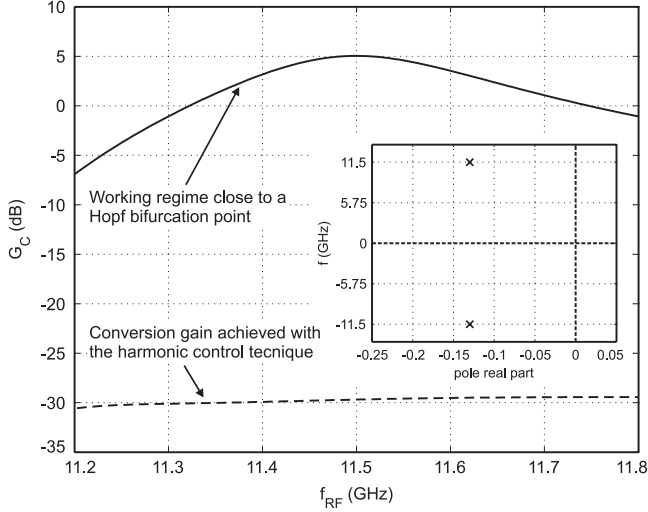


Figure 4. Dashed line: Conversion gain obtained with the harmonic control technique. Continuous line: Conversion gain achieved after creating a pair of complex conjugate poles with small negative real part and frequency $f = 11.5$ GHz. Inset: Representation of the created poles on the complex plane.

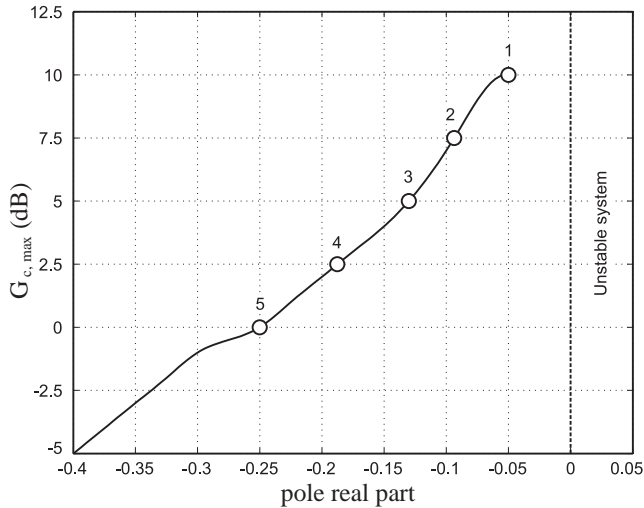


Figure 5. Maximum value of the conversion gain, $G_{c,max}$, as a function of the negative real part of the created complex conjugate poles. The harmonic content is ($V_o = 1.2$ V, $V_o^3 = 0.25$ V). The particular working points indicated with numbers from 1 to 5 will be referenced in the next sections.

Fig. 1).

The grey line in Fig. 4 shows the conversion gain around $f_{RF} = 11.5$ GHz of a circuit with harmonic content $V_o = 1.2$ V, $V_o^3 = 0.25$ V). The conversion gain achieved after creating a pair of complex conjugate poles, with negative real part $r_p \approx -0.13$ and frequency $f = 11.5$ GHz, is represented with black line. Note that the conversion gain improves about 30 dB.

The use of a multi-harmonic load based on an arbitrarily width modulated transmission line [19] provides a precise control over the position of the pair of complex conjugate poles created after reaching the condition expressed by (2) [7]. Therefore, several operating points, associated with different values of amplification, can be achieved. The maximum value of the conversion gain versus the negative real part of the created pole pair has been represented in Fig. 5. Since the magnitude of the amplification effect which is exploited in order to enlarge the magnitude of the input RF signal is greater for smaller values of $|r_p|$, the conversion gain of the HSOM increases as the real part of the pole pair approaches zero.

3.3. Independent Control of the Harmonic Content and the Working Point

The impedance of the transistor depends on the amplitude of the current flowing through it. Therefore, in order to set the operating regime close to a Hopf bifurcation point, the desired harmonic content is first selected, and then the parameters of the circuit are optimized to fulfill the condition given by (2).

In order to prove that the two factors that determine the conversion gain are controlled independently, three different HSOM circuits with different harmonic content have been designed. The amplitude of the fundamental component of the autonomous signal is the same in all the cases, $V_o = 1.2\text{ V}$, and the amplitude of its third harmonic component takes three different values $V_o^3 = \{10, 20, 30\}\text{ mV}$. As represented in Fig. 3, the conversion gain strongly depends on the value of V_o^3 , since it plays the role of local oscillator signal. The minimum value, $V_o^3 = 10\text{ mV}$ has been selected in order to ensure that the conversion gain after the optimization of the HSOM working point is not limited by the previous selection of the harmonic content. On the other hand, although the conversion gain is expected to increase with V_o^3 , it is very difficult to enlarge its magnitude over 30 mV . The amplitude of the fundamental harmonic component of the autonomous signal, $V_o = 1.2\text{ V}$, has been selected in order to ensure that the amplitude of V_o^3 can reach the value of 30 mV and to provide low ripple of the conversion gain frequency response (See Fig. 3).

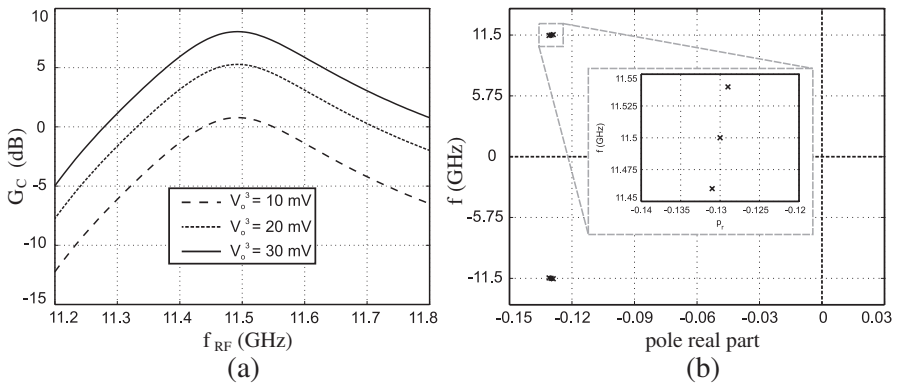


Figure 6. (a) Conversion gain versus the amplitude of the third harmonic component V_o^3 of the autonomous signal. (b) Position of the created poles.

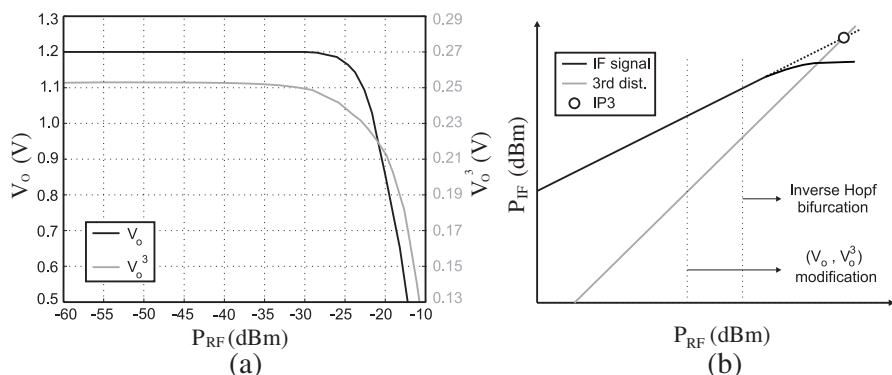


Figure 7. (a) Influence of the RF signal power P_{RF} on the harmonic content of the autonomous signal. Black line: V_o (left hand side y -axis). Grey line: V_o^3 (right hand side y -axis). (b) Classic method for determining the IP3.

After setting the harmonic content, a pair of complex conjugate poles has been created, with real part $r_p \approx -0.13$ and frequency $f \approx 11.5$ GHz, in the three circuits. Since the real part of the created poles is nearly the same, the operating regime of the three circuits is almost at the same distance from the Hopf bifurcation point, and the magnitude of the associated amplification effect is also the same in the three cases. The obtained conversion gain curves are represented in Fig. 6(a). As can be observed, the conversion gain increases with the amplitude of V_o^3 . The created poles are depicted in Fig. 6(b). Note that they are practically in the same position.

Thus, it is shown that the conversion gain of the HSOM depends on two different factors, namely, the harmonic content of the autonomous signal and the working regime close to a Hopf bifurcation point, and that these two factors can be independently controlled.

4. ANALYSIS OF THE LINEARITY OF THE HSOM

In order to analyze the linearity of the HSOM working as a mixer, the two figures of merit which are commonly used to characterize conventional amplifiers [8–10, 26, 27], and mixers [13, 15, 17, 28], namely, the 1 dB compression point and the third order interception point (IP3), will be calculated. In addition, an in-depth study of the influence of the harmonic content and the operating regime of the circuit on the linearity of the mixing operation will be performed.

In the case of the HSOM, the 1 dB compression and the IP3 cannot be directly calculated as in a conventional mixer. Due to the

autonomous nature of the circuit, the power of the input RF signal affects the frequency and the harmonic content of the autonomous signal. Therefore, for each considered value of the input RF signal power P_{RF} , the autonomous solution of the HSOM must be recalculated through an optimization process in which the optimization variables are the frequency f_o and the amplitude V_o of the autonomous signal. As can be observed in Fig. 7(a), the amplitudes of V_o and V_o^3 are almost constant when the input RF signal power is less than -25 dBm. From this value, the amplitudes of the fundamental and the third harmonic components of the autonomous signal decrease as the RF signal power increases. Hence, the power of the local oscillator signal, i.e., the third harmonic component of the autonomous signal, varies with the power of the input RF signal P_{RF} . In addition, if the power of the input signal reaches the value $P_{\text{RF}} \approx -10$ dBm, the amplitude of V_o quickly approaches zero, which means that the autonomous signal is extinguished via an inverse Hopf bifurcation [1].

4.1. Influence of the Harmonic Content

4.1.1. 1 dB Compression Point

The selected transistor provides a 1 dB compression point about $P_{1\text{ dB}} \approx 5$ dBm when it is used in conventional mixers and amplifiers, working with an input signal frequency about $f_{\text{RF}} \approx 12$ GHz. In this case, the 1 dB compression point cannot be reached. On the one hand, the amplitude of V_o^3 , which plays the role of local oscillator signal, is not constant if the power of the input RF signal is greater than -25 dBm. On the other hand, the autonomous signal is extinguished via an inverse Hopf bifurcation when the input RF signal power is above -10 dBm. Therefore, the theoretical value $P_{1\text{ dB}} = 5$ dBm cannot be reached because the mixing operation is not possible at that value of the RF signal power.

4.1.2. Third Order Distortion

As in the case of the 1 dB compression point, the third order interception point (IP3) cannot be calculated as in the case of standard mixers and amplifiers, because the 1 dB compression point cannot be reached and the value of V_o^3 depends on the power of the RF signal (see Fig. 7(b)).

In order to analyze the third order distortion versus the harmonic content of the autonomous signal, an input RF signal composed of two tones with the same power P_{RF} and frequencies $f_{\text{RF},1} = 11.5$ GHz and $f_{\text{RF},2} = 11.51$ GHz is provided to the circuit. Next, the difference

$P_{\text{delta}} = P_{\text{IF}} - P_{3\text{rd, dist}}$ between the power of the output IF signal, with frequency $f_{\text{IF}} = f_{\text{RF}, 1} - 3f_o$ and the signal which causes the third order distortion, with frequency $f_{3\text{rd dist}} = (2f_{\text{RF}, 2} - f_{\text{RF}, 1}) - 3f_o$, is computed for different values of P_{RF} . Note that, for each value of P_{RF} , the frequency f_o and the amplitude V_o of the autonomous signal must be recalculated.

Figure 8 shows the obtained value of P_{δ} for different values of the harmonic content (V_o, V_o^3) of the autonomous signal and the RF signal power. As can be observed from Figs. 8(a), 8(b) and 8(c), when the amplitude of the fundamental harmonic component of the autonomous signal V_o is less than 1.2 V, the behavior of the different circuits is almost the same. The power difference P_{δ} is practically constant for all the pairs (V_o, V_o^3) and, in the worst considered case, with $P_{\text{RF}} = -40$ dBm, its value is about 60 dB, which means that the HSOM circuit provides low third order distortion. Note that the distortion considerably increases when V_o^3 is larger than 0.4 V. On the other hand, if the amplitude of the fundamental harmonic component of the autonomous signal is above 1.2 V, the value of V_o^3 has a greater influence on P_{δ} . In this case, the third order distortion increases for V_o^3 values between 0.3 and 0.4 V, and decreases as V_o^3 grows above 0.4 V. Although the distortion values obtained with $V_o^3 > 0.5$ V are similar to those provided by $V_o^3 \approx 0.3$ V, the latter case is preferred, because that harmonic content can be easily achieved.

Combining the data represented in Figs. 8 and 3, the optimum pair (V_o, V_o^3) for each particular application can be selected, in order to reach a trade-off between the conversion gain and the maximum allowed third order distortion.

4.2. Influence of the Working Regime

In order to analyze the influence of the proximity of the working regime of the HSOM to the Hopf bifurcation point on the linearity of the mixing operation, the 1 dB compression point and the third order distortion P_{δ} will be calculated for different circuits, with the same harmonic content, operating at different distances from the Hopf bifurcation point.

4.2.1. 1 dB Compression Point

The high flexibility of the multi-harmonic load based on an arbitrarily width modulated transmission line allows the precise control of the working point of the circuit. In this case, several circuits with the same harmonic content ($V_o = 1.2$ V, $V_o^3 = 0.25$ V) working at different distances from the Hopf bifurcation point have been designed.

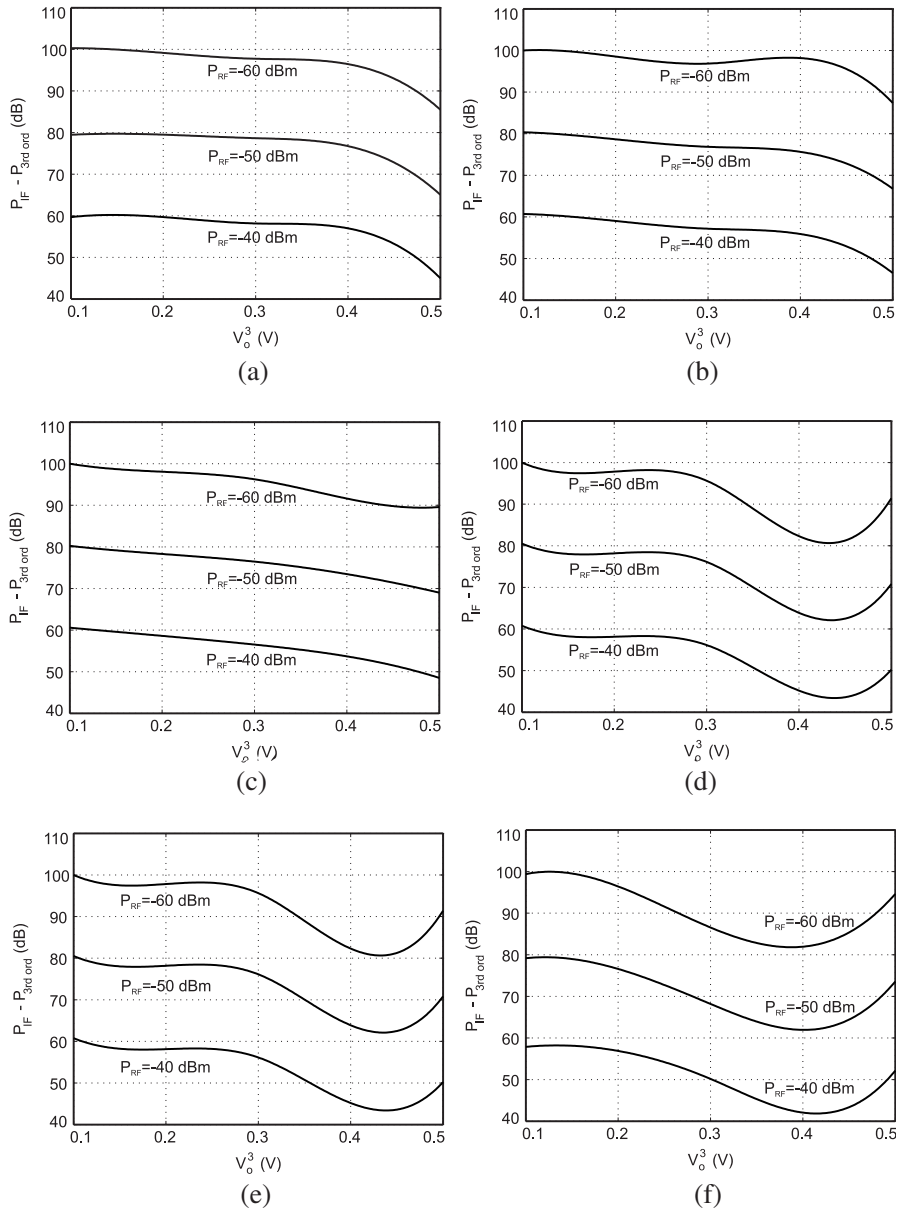


Figure 8. Power difference P_δ between the IF signal and the third order distortion. (a) $V_o = 1$ V. (b) $V_o = 1.1$ V. (c) $V_o = 1.2$ V. (d) $V_o = 1.3$ V. (e) $V_o = 1.4$ V. (f) $V_o = 1.5$ V.

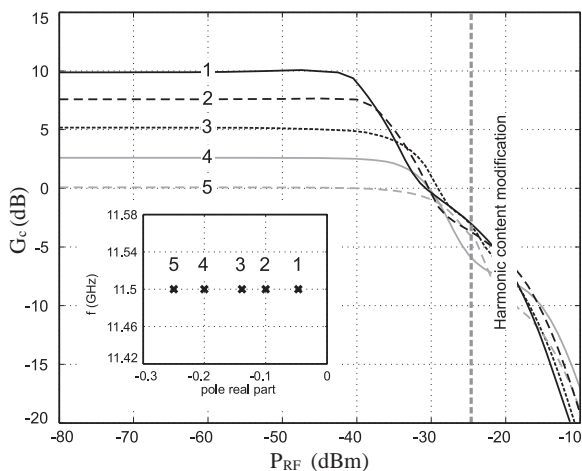


Figure 9. Influence of the working point of the HSOM on the 1 dB compression point. Inset: Created pairs of poles corresponding to the considered five different operating regimes, which are identified by the numbers from 1 to 5.

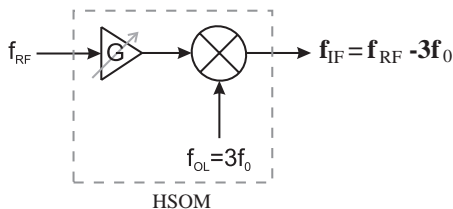


Figure 10. Equivalent circuit of the HSOM working close to a Hopf bifurcation point.

Therefore, the conversion gain of each HSOM is given by the value of the negative real part of the created complex conjugate pair of poles. The 1 dB compression point is calculated by sweeping the value of the input RF signal power P_{RF} and calculating the power of the IF output signal. Note that, for each value of P_{RF} , the parameters of the autonomous solution must be recalculated before determining the conversion gain.

The conversion gain of the HSOM circuits with different operating regimes, calculated at the center of the working band as G_c (dB) = P_{IF} (dBm) - P_{RF} (dBm) has been represented in Fig. 9. Note that the 1 dB compression point reduces in the same proportion as the maximum conversion gain increases. This is due to the fact that the

amplification effect associated with the working point of the HSOM affects the input RF signal before the mixing operation. Hence, as the distance of the created pair of poles to the imaginary axis of the complex plane is reduced, the magnitude of the amplification effect is greater and the power of the RF input signal involved in the mixing process is also enlarged.

From the data represented in Fig. 9, the HSOM working close to a Hopf bifurcation point can be represented through the equivalent circuit represented in Fig. 10. It is composed by a harmonic self-oscillating mixer, whose features depend on the harmonic content of the autonomous signal and by an ideal amplifier which affects the input RF signal. The gain of this amplifier is conditioned by the distance of the working regime of the HSOM to the Hopf bifurcation point and, for relatively low values of P_{RF} , it does not depend on the input RF signal power. Therefore, the value of the 1 dB compression point is only determined by the harmonic self-oscillating mixer.

4.2.2. Third Order Distortion

Finally, the power difference P_δ between the output IF signal and that which causes the third order distortion has been calculated, at the frequency for which the largest conversion gain is obtained. The resulting data have been represented in Fig. 11. The value of P_δ

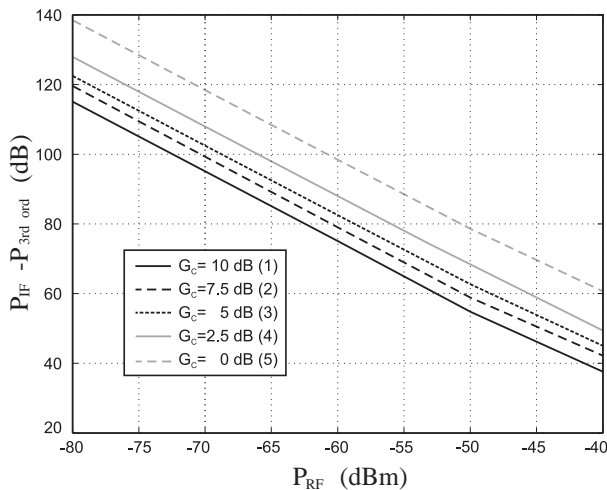


Figure 11. Influence of the working regime on the third order distortion. The numbers in brackets correspond to the different working regimes considered in Figs. 5 and 9.

decreases as the maximum conversion gain grows, which means that the third order distortion increases as the distance to the Hopf bifurcation point is reduced. Anyway, for a maximum value of the conversion gain about $G_c = 5$ dB, P_δ is bigger than 50 dB for all the considered values of the input RF signal power. Note also that, when the power of the input RF signal is lower than -50 dBm, all the traces depicted in Fig. 11 are straight lines with -2 dB slope, which means that when the power of the RF signal increases 1 dB, the power of the IF signal also increases 1 dB, while that of the third order distortion signal increases 3 dB. Therefore, the mixer is working in a linear regime, despite the high amplification associated with the working point.

5. CONCLUSIONS

The conversion gain of a Harmonic Self-Oscillating Mixer has been analyzed versus the harmonic content of the autonomous signal and it has been considerably improved through the selection of an adequate working regime, close to a Hopf bifurcation point. The linearity of the mixing operation has been characterized through the analysis of the influence of the two considered factors in the 1 dB compression point and the third order distortion. It has been shown that the 1 dB compression point reduces and the third order distortion worsens as the maximum gain increases, due to the generated amplification effect. However, it can be assumed that the mixer works in a linear zone when the input RF signal power is below -40 dBm, which ensures that the HSOM can be used in front-end stages of microwave receivers. The data collected from the presented analysis can be used to select the optimum harmonic content and working regime for each particular application, in order to reach a trade-off between IF signal distortion and conversion gain.

ACKNOWLEDGMENT

This work has been supported by the “Ministerio de Ciencia e Innovación” of Spain and “FEDER”, under projects IPT-2011-0951-390000 (TECNIGRAF), TEC2011-24492 (ISCAT), TEC2008-01638 (INVEMTA), “CONSOLIDER-INGENIO CSD2008-00068” (TERASENSE) and grant AP2009-0438, by the “Plan de Ciencia y Tecnología” (PCTI/FEDER-FSE) of the “Gobierno del Principado de Asturias”, under projects EQUIP08-06, FC09-COF09-12, EQUIP10-31 and PC10-06, and grant BP10-031, and by the “Catedra Telefonica-Universidad de Oviedo”.

REFERENCES

1. Ver Hoeye, S., L. Zurdo, and A. Suarez, "New nonlinear design tools for self-oscillating mixers," *IEEE Microwave and Wireless Components Letters*, Vol. 11, No. 8, 337–339, 2001.
2. Ver Hoeye, S., F. Ramirez, and A. Suarez, "Nonlinear optimization tools for the design of high-efficiency microwave oscillators," *IEEE Microwave and Wireless Components Letters*, Vol. 14, No. 5, 189–191, 2004.
3. Herran, L. F., S. Ver Hoeye, and F. Las Heras, "Nonlinear optimization tools for the design of microwave high-conversion gain harmonic self-oscillating mixers," *IEEE Microwave and Wireless Components Letters*, Vol. 16, No. 1, 16–18, 2006.
4. Makeeva, G. S., O. A. Golovanov, and M. Pardavi-Horvath, "Mathematical modeling of nonlinear waves and oscillations in gyromagnetic structures by bifurcation theory methods," *Journal of Electromagnetic Waves and Applications*, Vol. 20, No. 11, 1503–1510, 2006.
5. Fernandez, M., S. Ver Hoeye, L. F. Herran, and F. Las Heras, "Nonlinear optimization of wide-band harmonic self-oscillating mixers," *IEEE Microwave and Wireless Components Letters*, Vol. 18, No. 5, 347–349, 2008.
6. Fernandez, M., S. Ver Hoeye, L. F. Herran, C. Vazquez, and F. Las Heras, "Design of high-gain wide-band harmonic self oscillating mixers," *Proceedings of Workshop on Integrated Nonlinear and Millimetre-Wave Circuits (INMMIC)*, Vol. 1, No. 1, 57–60, 2008.
7. Fernandez, M., S. Ver Hoeye, C. Vazquez, G. Hotopan, R. Cambor, and F. Las Heras, "Optimization of the synchronization bandwidth of rationally synchronized oscillators based on bifurcation control," *Progress In Electromagnetics Research*, Vol. 119, 299–313, 2011.
8. Yoon, J., H. Seo, I. Choi, and B. Kim, "Wideband LNA using a negative g_m cell for improvement of linearity and noise figure," *Progress In Electromagnetics Research*, Vol. 105, 253–272, 2010.
9. Choi, H., Y. Jeong, C. D. Kim, and J. S. Kenney, "Bandwidth enhancement of an analog feedback amplifier by employing a negative group delay circuit," *Progress In Electromagnetics Research*, Vol. 105, 253–272, 2010.
10. El Maazouzi, L., A. Mediavilla, and P. Colantonio, "A contribution to linearity improvement of a highly efficient PA for WIMAX applications," *Progress In Electromagnetics Research*, Vol. 119, 59–84, 2011.

11. Guo, B. and G. Wen, "Periodic time-varying noise in current-commutating CMOS mixers," *Progress In Electromagnetics Research*, Vol. 117, 283–298, 2011.
12. Park, C., H. Seo, and B. Kim, "A noise optimized passive mixer for charge-domain sampling applications," *Journal of Electromagnetic Waves and Applications*, Vol. 23, Nos. 14–15, 1909–1917, 2009.
13. Guo, J., Z. Xu, C. Qian, and W. Dou, "Design of a microstrip balanced mixer for satellite communication," *Progress In Electromagnetics Research*, Vol. 115, 289–301, 2011.
14. Lee, Y.-C., Y.-H. Chang, S.-H. Hung, W.-C. Chien, C.-C. Su, C.-C. Hung, C.-M. Lin, and Y.-H. Wang, "A single-balanced quadruple subharmonic mixer with a compact IF extraction," *Progress In Electromagnetics Research Letters*, Vol. 24, 159–167, 2011.
15. Lee, Y.-C., C.-M. Lin, S.-H. Hung, C.-C. Su, and Y.-H. Wang, "A broadband doubly balanced monolithic ring mixer with a compact intermediate frequency (IF) extraction," *Progress In Electromagnetics Research Letters*, Vol. 20, 175–184, 2011.
16. Zhang, B., Y. Fan, X. F. Chen, and F. Q. Zhong, "An improved 110-130-GHz fix-tuned subharmonic mixer with compact microstrip resonant cell structure," *Journal of Electromagnetic Waves and Applications*, Vol. 25, Nos. 2–3, 411–420, 2011.
17. Chien, W.-C., C.-M. Lin, Y.-H. Chang, and Y.-H. Wang, "A 9–21 GHz miniature monolithic image reject mixer in 0.18- μm CMOS technology," *Progress In Electromagnetics Research Letters*, Vol. 17, 105–114, 2010.
18. Garcia, J. A., L. Cabria, R. Marante, L. Rizo, and A. Mediavilla, "An unbiased dual-mode mixing antenna for wireless transponders," *Progress In Electromagnetics Research*, Vol. 102, 1–14, 2010.
19. Ver Hoeye, S., C. Vazquez, M. Fernandez, L. F. Herran, and F. Las Heras, "Multi-harmonic DC-bias network based on arbitrarily width modulated microstrip line," *Progress In Electromagnetics Research Letters*, Vol. 11, 119–128, 2009.
20. Gonzalez-Posadas, V., J. L. Jimenez-Martin, A. Parra-Cerrada, D. Segovia-Vargas, and L. E. Garcia-Munoz, "Oscillator accurate linear analysis and design. Classic linear methods review and comments," *Progress In Electromagnetics Research*, Vol. 118, 89–116, 2011.
21. Vahdati, H. and A. Abdipour, "Nonlinear stability analysis of an oscillator using the periodic averaging method," *Progress In Electromagnetics Research*, Vol. 79, 179–193, 2008.

22. Vahdati, H. and A. Abdipour, "Nonlinear stability analysis of an oscillator with distributed element resonator," *Progress In Electromagnetics Research*, Vol. 80, 241–252, 2008.
23. Fernandez, M., S. Ver Hoeye, C. Vazquez, G. R. Hotopan, R. Camblor, and F. Las Heras, "Design and analysis of a multi-carrier Tx-Rx system based on rationally synchronized oscillators for localization applications," *Progress In Electromagnetics Research*, Vol. 120, 1–16, 2011.
24. Ver Hoeye, S., A. Suarez, and S. Sancho, "Analysis of noise effects on the nonlinear dynamics of synchronized oscillators," *IEEE Microwave and Wireless Components Letters*, Vol. 11, No. 9, 376–378, 2001.
25. Jugo, J., J. Portilla, A. Anakabe, A. Suarez, and J. M. Collantes, "Closed-loop stability analysis of microwave amplifiers," *IEE Electronics Letters*, Vol. 37, No. 4, 226–228, 2001.
26. Zhang, B., "A D-band power amplifier with 30-GHz bandwidth and 4.5-DBM P_{sat} for high-speed communication system," *Progress In Electromagnetics Research*, Vol. 107, 161–178, 2010.
27. Kung, F. and S.-K. Wong, "A WIMEDIA compliant CMOS RF power amplifier for ultra-wideband (UWB) transmitter," *Progress In Electromagnetics Research*, Vol. 112, 329–347, 2011.
28. Wei, H. C., R. M. Weng, and S. Y. Li, "A broadband high linearity and isolation down-conversion mixer for WIMAX applications," *Journal of Electromagnetic Waves and Applications*, Vol. 23, Nos. 11–12, 1555–1565, 2009.